FINITE ELEMENT ANALYSIS OF THICK CIRCULAR PLATES ON ELASTIC FOUNDATIONS

Dr. Riyadh J. Aziz
Assistant Professor
Al-Nahrain University

Dr. Adel A. Al-Azzawi
Lecturer
Al-Nahrain University

Mustafa H. Al-Allaf
Researcher
Al-Nahrain University

ABSTRACT

This paper deals with the linear elastic behavior of thick circular plates on Winkler type elastic foundations with both compressional and tangential resistances. The finite element method with different isoparametric thick plate and brick finite elements are used to solve problems, which were previously solved by the finite difference method. Good agreement was noticed between the different methods

KEYWORDS

Finite element, Thick circular plates, Winkler foundations.

NOMENCLUTURES

Symbols	Description
a	Radius of circular plate.
[B]	Strain-displacement matrix.
c^2	Correction factor for transverse shear.
D	Flexural rigidities of isotropic plates.
[D]	Matrix of elastic constants.
E	Modulus of elasticity of isotropic plates.
F_r,F_θ	Horizontal frictional forces in r and θ directions.
G	Shearing modulus for isotropic plates.
h	Plate thickness.
[J]	Jacobian matrix.
[K]	Element stiffness matrix for plate-foundation system.
$[K_f]$	Stiffness matrix for the foundation.
$[K_p]$	Stiffness matrix for the plate.
K_r,K_θ,K_z	Moduli of subgrade reactions in r, θ and z directions.
M_r, M_θ	Bending moments in rz and θz planes (per unit width).
$M_{r\theta}$	Twisting moments (per unit width) in r and θ direction.
[N]	Matrix contains the interpolation shape functions
N_1,N_2…	Shape functions.
P	Applied concentrated load.

NOMENCLUTURES- Continued

Symbols	Description
Q_r, Q_θ	Transverse shearing force per unit area width in r and θ direction.
$q(r,\theta)$	Transverse load per unit area in r, θ direction.
u,v	Displacements in r and θ directions
w	Displacement in z-direction.
w_c	Displacement in z-direction at centre of plate.
Δ	nodal displacements.
$\{\delta\}$	Total displacements in the system.
ε_r, ε_θ, ε_z	Normal strains in r, θ and z directions.
ξ,ή	Local coordinates system.
μ_r, μ_θ	External moments per unit area in rz and θz-planes
ν	Poisson ratio of isotropic material.
ψ_r,ψ_θ	Rotations of the transverse sections in rz and θz -planes.
$\gamma_{r\theta}$,γ_{rz},$\gamma_{\theta z}$	Engineering shearing strains in rθ, rz and θz-planes.
$\tau_{r\theta}$,$\tau_{rz,}\tau_{\theta z}$	Shearing stresses in rθ, rz and θz- planes.
σ_r,σ_θ,σ_z	Normal stresses in r, θ and z directions.

INTRODUCTION

Circular plates are plane structures of constant or variable thickness and bounded by two surfaces which are the top and bottom faces of the plate and by curved transverse edges. They can

sustain generalized transverse loads by the development of bending and twisting moments and by transverse shearing forces in the transverse sections of the plate.

The problem of thick circular plates on elastic foundations was investigated by Naghdi and Rowely (1953)[10]. They extended Reissner's theory of thick plates to include the effect of elastic foundations that would behave according to the classical Winkler assumption. Only problems of axially symmetric bending of thick infinite plates on Winkler foundations were considered.

Fredrick (1956) modified the basic equations of Reissner's theory to include an elastic foundation in the same manner of Naghdi and Rowely. Fredrick presented the solution of axisymmteric and asymmetric isotropic thick circular plates on elastic foundations using Bessel functions. The results were given in tables for different plate thickness to radius ratios and the comparisons between an infinite and a finite circular plate on an elastic foundation were shown in graphical plots [4].

Perakatte and Lehnhoff (1971) used Mindlin's linear shear deformation theory of elastic isotropic thick plate for solving axially symmetric deformation of uniform circular plates with static loads. The flexural equilibrium equations are solved for (12) specific cases of loading and boundary conditions. The solutions and numerical

results are presented in non-dimensional forms with a shear correction factor (c^2=0.86) [11].

Many investigators have presented higher-order theories for thick plates. Schmidt (1977) and Levinson (1980) presented a theory for thick isotropic plates of uniform thickness including transverse shearing deformations. In this theory, the cross sections are allowed to warp in such a fashion that they remain normal to the shear free faces of the plate (thus not requiring a transverse shear correction factor). Mindlin's plate theory and the theory developed by Schmidt and Levinson lead to the same results if the shear correction factor in Mindlin's theory is taken to be (c^2=5/6) [7,14].

Liu and Solecki (2001) studied an infinite thick plate on Winkler foundation. The effect of shear between the plate and the foundation on the deflection and the stresses was analyzed. It is assumed that the foundation has stiffness K_{fs} (the force needed to produce a unit displacement per area) and reacts in compression as well as tension. The effect of a concentrated normal unit force is investigated. The solution is based on Airy stress function formulation. In particular, the following two special cases are studied; first deflections of a relatively thin plate are compared to the results obtained by Timoshenko and Woinowsky Krieger, which give excellent correlation. Second when the thickness becoming

infinite, the solution of Boussinesq's problems is readily recovered [8].

In this paper, Mindlin's thick plate theory is used to analyze thick circular plates on elastic foundations subjected to generalized loadings which are externally distributed shearing forces at top and bottom faces of the plate and distributed moments, in addition to the usually applied transverse loads. The transverse section has three degrees of the freedom (the deflection w and the two rotations of the normal line to the middle plane ψ_r and ψ_θ in case of plate bending element) or (the deflection w and the displacements u and v in case of brick elements). The elastic foundation is represented by a Winkler model, which is assumed that the base is consisting of closely spaced independent linear springs for normal and tangential reactions as shown in figure (1).

FINITE ELEMENT MODEL

The two-dimensional isoparametric thick plate element in local coordinates ξ and η has n nodes [5]. Each node i has three degrees of freedom. They are (w_i, ψ_{ri}, $\psi_{\theta i}$) in polar cylindrical coordinates. Thus, the element degrees of freedom may be listed in the vector (or column matrix).

$$\{\delta^e\} = [w_1, \psi_{r1}, \psi_{\theta 1}, \ldots\ldots\ldots\ldots w_{ni}, \psi_{rn}, \psi_{\theta n}]$$

The family of elements and polynomials are indicated in figure (2).

For the eight-node isoparametric quadrilateral element, the shape functions are:

$$\left.\begin{aligned}
N_1 &= (1-\xi)(1-\eta)(1+\xi+\eta)/4 \\
N_2 &= (1-\xi^2)(1-\eta)/2 \\
N_3 &= (1+\xi)(1-\eta)(\xi-\eta-1)/4 \\
N_4 &= (1+\xi)(1-\eta^2)/2 \\
N_5 &= (1+\xi)(1+\eta)(\xi+\eta-1)/4 \\
N_6 &= (1-\xi^2)(1+\eta)(-\xi+\eta-1)/4 \\
N_7 &= (1-\xi)(1-\eta)(-\xi+\eta-1)/4 \\
N_8 &= (1-\xi)(1-\eta^2)/2
\end{aligned}\right\} \quad \text{... (1)}$$

The degrees of freedom in polar cylindrical coordinate $(w_i, \psi_{ri}, \psi_{\theta i})$ can be defined as:

$$\left.\begin{aligned}
w(\xi,\eta) &= \sum_{i=1}^{n} N_i . w_i \\
\psi_r(\xi,\eta) &= \sum_{i=1}^{n} N_i . \psi_{ri} \\
\psi_\theta(\xi,\eta) &= \sum_{i=1}^{n} N_i . \psi_{\theta i}
\end{aligned}\right\} \quad \text{... (2)}$$

The r and θ coordinate can be defined as:

$$\left.\begin{aligned} r(\xi) &= \sum_{i=1}^{n} N_i . r_i \\ \theta(\xi) &= \sum_{i=1}^{n} N_i \theta_i \end{aligned}\right\} \qquad \text{... (3)}$$

Thus, the geometry and the assumed displacement field are described in a similar fashion using the shape functions and the nodal values (thus, the name of isoparametric element is given).

The Jacobian matrix [J] is obtained from the following expression:

$$[J] = \begin{bmatrix} \frac{\partial r}{\partial \xi} & \frac{\partial \theta}{\partial \xi} \\ \frac{\partial r}{\partial \eta} & \frac{\partial \theta}{\partial \eta} \end{bmatrix} = \sum_{i=1}^{n} \begin{bmatrix} \frac{\partial N_i}{\partial \xi} r_i & \frac{\partial N_i}{\partial \xi} \theta_i \\ \frac{\partial N_i}{\partial \eta} r_i & \frac{\partial N_i}{\partial \eta} \theta_i \end{bmatrix} \qquad \text{... (4)}$$

The inverse of Jacobian matrix $[J]^{-1}$can be readily obtained by using standard matrix inversion techniques:

$$[J]^{-1} = \begin{bmatrix} \frac{\partial \xi}{\partial r} & \frac{\partial \eta}{\partial r} \\ \frac{\partial \xi}{\partial \theta} & \frac{\partial \eta}{\partial \theta} \end{bmatrix} = \frac{1}{\det J} \begin{bmatrix} \frac{\partial \theta}{\partial \eta} & -\frac{\partial \theta}{\partial \xi} \\ -\frac{\partial r}{\partial \eta} & \frac{\partial r}{\partial \xi} \end{bmatrix} \qquad \text{... (5)}$$

The shape function derivatives are calculated from the expression:

$$\left.\begin{aligned}\frac{\partial N_i}{\partial r} &= \frac{\partial N_i}{\partial \xi}\ \frac{\partial \xi}{\partial r} + \frac{\partial N_i}{\partial \eta}\ \frac{\partial \eta}{\partial r}\\ \frac{\partial N_i}{\partial \theta} &= \frac{\partial N_i}{\partial \xi}\ \frac{\partial \xi}{\partial \theta} + \frac{\partial N_i}{\partial \eta}\ \frac{\partial \eta}{\partial \theta}\end{aligned}\right\} \qquad \text{... (6)}$$

where $\frac{\partial \xi}{\partial r}, \frac{\partial \eta}{\partial r}, \frac{\partial \xi}{\partial \theta}$ and $\frac{\partial \eta}{\partial \theta}$ are obtained from $[J]^{-1}$.

The strains in polar cylindrical coordinates are obtained:

$$\begin{Bmatrix}\varepsilon_r\\ \varepsilon_\theta\\ \gamma_{r\theta}\\ \gamma_{rz}\\ \gamma_{\theta z}\end{Bmatrix} = \sum_{i=1}^{n}\begin{bmatrix} 0 & -\frac{\partial N_i}{\partial r} & 0\\ 0 & \frac{N_i}{r} & \frac{1}{r}\frac{\partial N_i}{\partial \theta}\\ 0 & \frac{1}{r}\frac{\partial N_i}{\partial \theta} & \frac{\partial N_i}{\partial r} - \frac{N_i}{r}\\ \frac{\partial N_i}{\partial r} & -N_i & 0\\ \frac{\partial N_i}{r\partial \theta} & 0 & -N_i\end{bmatrix}\begin{Bmatrix} w_i\\ \psi_{ri}\\ \psi_{\theta i}\end{Bmatrix} \qquad \text{... (7)}$$

or

$$\{\varepsilon^e\} = \sum_{i=1}^{n}[B_i]\{\delta^e\} \qquad \text{... (8)}$$

The strain matrix $[B_i]$ contains shape function derivatives which may be calculated from the Expression (6) and r, which may be calculated at the Gauss point, coordinates from Expression (3)

The generalized stress-strain relationship for a plate of thick isotropic plate in polar cylindrical coordinates is written as:

$$\begin{Bmatrix} M_r \\ M_\theta \\ M_{r\theta} \\ Q_r \\ Q_\theta \end{Bmatrix} = \begin{bmatrix} D & \nu.D & 0 & 0 & 0 \\ \nu.D & D & 0 & 0 & 0 \\ 0 & 0 & \frac{(1-\nu)D}{2} & 0 & 0 \\ 0 & 0 & 0 & c^2.Gh & 0 \\ 0 & 0 & 0 & 0 & c^2.Gh \end{bmatrix} \begin{Bmatrix} \varepsilon_r \\ \varepsilon_\theta \\ \gamma_{r\theta} \\ \gamma_{rz} \\ \gamma_{\theta z} \end{Bmatrix} \qquad \text{... (9)}$$

where $D=E.h^3/ 12(1-\nu^2)$ is the flexural rigidity of the section of the plate.

or

$$\{\sigma^e\} = [D]\ \{\varepsilon^e\} \qquad \text{... (10)}$$

where [D] is the matrix of elastic constants for elastic thick plate in polar cylindrical coordinates.

Similarly, the stress at any point within the element for a plate can be expressed as:

$$\{\sigma^e\} = [D][B]\{\delta^e\} = [S]\{\delta^e\} \qquad \text{... (11)}$$

The element stiffness matrix for isotropic elastic plates in polar coordinates is given as:

$$\left[K_p\right]=\sum_{i=1}^{n}\int_{-1}^{+1}\int_{-1}^{+1}[B_i]^T[D][B_i]r\det J d\xi d\eta \qquad \text{... (12)}$$

where [D] is given in equation (9) for isotropic plates.

For a foundation represented by Winkler model for both compressional and frictional resistances for a thick plate element, the stiffness matrix:

$$[K_f]=\begin{bmatrix} [R_w] & 0 & 0 & 0 & 0 \\ 0 & [R_w] & 0 & 0 & 0 \\ 0 & 0 & [R_w] & 0 & 0 \\ 0 & 0 & 0 & [R_w] & 0 \\ 0 & 0 & 0 & 0 & [R_w] \end{bmatrix}_{nxn} \qquad \text{... (13)}$$

where,

$$[R_w]=\begin{bmatrix} K_{f1} & 0 & 0 \\ 0 & K_{f2} & 0 \\ 0 & 0 & K_{f3} \end{bmatrix}$$

In polar cylindrical coordinates:

$$K_{f_1}=\int_{-1}^{+1}\int_{-1}^{+1}N_i.K_z.r\det J.d\xi d\eta$$

$$K_{f_2} = \int_{-1}^{+1}\int_{-1}^{+1} N_i . \frac{K_r . h^2}{4} r . detJ . d\xi . d\eta \quad \text{... (14)}$$

$$K_{f3} = \int_{-1}^{+1}\int_{-1}^{+1} N_i . \frac{K_\theta . h^2}{4} r . detJ . d\xi . d\eta$$

The element stiffness matrix for the plate–foundation system is given as:

$$[K] = [K_P] + [K_f] \quad \text{... (15)}$$

The twenty-node isoparametric brick element shown in figure (3) is used in the analysis. The element in local coordinates (ξ, η, ζ) at node i has the nodal displacements u_i, v_i and w_i respectively [6]. Thus,

$$\{\delta^e\} = [w_1, u_1, v_1, ..., w_n, u_n, v_n]$$

The isoparametric definition of the brick element is:

$$\left.\begin{aligned} u(\xi,\eta,\zeta) &= \sum_{i=1}^{n} N_i(\xi,\eta,\zeta).u_i \\ v(\xi,\eta,\zeta) &= \sum_{i=1}^{n} N_i(\xi,\eta,\zeta).v_i \\ w(\xi,\eta,\zeta) &= \sum_{i=1}^{n} N_i(\xi,\eta,\zeta).w_i \end{aligned}\right\} \quad \text{... (16)}$$

where, $N_i(\xi,\eta,\zeta)$ represents the shape functions for the global coordinates $x(\xi,\eta,\zeta)$,$y(\xi,\eta,\zeta)$, $z(\xi,\eta,\zeta)$ at node i. The shape functions for twenty node elements are shown in Table (1).

In polar cylindrical coordinates:

$$\left.\begin{aligned} r(\xi,\eta,\zeta) &= \sum_{i=1}^{n} N_i(\xi,\eta,\zeta).r_i \\ \theta(\xi,\eta,\zeta) &= \sum_{i=1}^{n} N_i(\xi,\eta,\zeta).\theta_i \\ z(\xi,\eta,\zeta) &= \sum_{i=1}^{n} N_i(\xi,\eta,\zeta).z_i \end{aligned}\right\} \quad \text{... (17)}$$

where r, θ and z are the polar cylindrical coordinates at any point and r_i, θ_i and z_i are the nodal coordinates(for node i)..

The Jacobian matrix i can be expressed as:

$$[J]=\begin{bmatrix} \frac{\partial r}{\partial \xi} & \frac{\partial \theta}{\partial \xi} & \frac{\partial z}{\partial \xi} \\ \frac{\partial r}{\partial \eta} & \frac{\partial \theta}{\partial \eta} & \frac{\partial z}{\partial \eta} \\ \frac{\partial r}{\partial \zeta} & \frac{\partial \theta}{\partial \zeta} & \frac{\partial z}{\partial \zeta} \end{bmatrix} \quad \text{... (18)}$$

By substituting of Equation (17) in Equation (18), the Jacobian matrix [J] is constructed in the form:

$$[J]=\sum_{i=1}^{n}\begin{bmatrix}\frac{\partial N_i}{\partial \xi} r_i & \frac{\partial N_i}{\partial \xi}\theta_i & \frac{\partial N_i}{\partial \xi} z_i \\ \frac{\partial N_i}{\partial \eta} r_i & \frac{\partial N_i}{\partial \eta}\theta_i & \frac{\partial N_i}{\partial \eta} z_i \\ \frac{\partial N_i}{\partial \zeta} r_i & \frac{\partial N_i}{\partial \zeta}\theta_i & \frac{\partial N_i}{\partial \zeta} z_i \end{bmatrix} \quad \text{... (19)}$$

The inverse of Jacobian matrix can be written as:

$$[J]^{-1}=\sum_{i=1}^{n}\begin{bmatrix}\frac{\partial \xi}{\partial r} & \frac{\partial \eta}{\partial r} & \frac{\partial \zeta}{\partial r} \\ \frac{\partial \xi}{\partial \theta} & \frac{\partial \eta}{\partial \theta} & \frac{\partial \zeta}{\partial \theta} \\ \frac{\partial \xi}{\partial z} & \frac{\partial \eta}{\partial z} & \frac{\partial \zeta}{\partial z} \end{bmatrix} \quad \text{... (20)}$$

The strain matrix in polar cylindrical coordinates can be written as:

$$\begin{Bmatrix} \varepsilon_r \\ \varepsilon_\theta \\ \varepsilon_z \\ \gamma_{r\theta} \\ \gamma_{\theta z} \\ \gamma_{zr} \end{Bmatrix} = \sum_{i=1}^{n} \begin{bmatrix} \frac{\partial N_i}{\partial r} & 0 & 0 \\ \frac{N_i}{r} & \frac{1}{r}\frac{\partial N_i}{\partial \theta} & 0 \\ 0 & 0 & \frac{\partial N_i}{\partial z} \\ \frac{1}{r}\frac{\partial N_i}{\partial \theta} & \frac{\partial N_i}{\partial r} - \frac{N_i}{r} & 0 \\ \frac{\partial N_i}{\partial z} & 0 & \frac{1}{r}\frac{\partial N_i}{\partial \theta} \\ 0 & \frac{\partial N_i}{\partial z} & \frac{\partial N_i}{\partial r} \end{bmatrix} \begin{Bmatrix} u_i \\ v_i \\ w_i \end{Bmatrix} \quad \text{... (21)}$$

or

$$\{\varepsilon^e\} = \sum_{i=1}^{n} [B_i].\{\delta^e\} \quad \text{... (22)}$$

The strain matrix $[B_i]$ contains the shape function derivatives

In polar cylindrical coordinates the stresses are calculated from the expression:

$$\begin{Bmatrix} \sigma_r \\ \sigma_\theta \\ \sigma_z \\ \tau_{r\theta} \\ \tau_{rz} \\ \tau_{\theta z} \end{Bmatrix} = \begin{bmatrix} D_1 & D_2 & D_2 & 0 & 0 & 0 \\ D_2 & D_1 & D_2 & 0 & 0 & 0 \\ D_2 & D_2 & D_1 & 0 & 0 & 0 \\ 0 & 0 & 0 & G & 0 & 0 \\ 0 & 0 & 0 & 0 & G & 0 \\ 0 & 0 & 0 & 0 & 0 & G \end{bmatrix} \begin{Bmatrix} \varepsilon_r \\ \varepsilon_\theta \\ \varepsilon_z \\ \gamma_{r\theta} \\ \gamma_{rz} \\ \gamma_{\theta z} \end{Bmatrix} \quad \text{... (23)}$$

where, $D_1 = \frac{E.(1-\nu)}{(1+\nu)(1-2\nu)}, D_2 = \frac{E.\nu}{(1+\nu)(1-2\nu)}$ and $G = \frac{E}{2(1+\nu)}$

in which D_1 and D_2 are the elastic constant for the isotropic elastic material and G is the shear modulus for the isotropic material.

or

$$\{\sigma^e\} = [D]\{\varepsilon^e\} \quad \text{... (24)}$$

The element stiffness matrix in polar cylindrical coordinates is given as:

$$[K_p] = \sum_{i=1}^{n} \int_{-1}^{+1}\int_{-1}^{+1}\int_{-1}^{+1} [B_i]^T [D][B_i] r \, \det J \, d\xi d\eta d\zeta \quad \text{... (25)}$$

where D is the elastic constant matrix given in Equations (23).

For a foundation represented by Winkler model for the both compressional and frictional resistances on a brick element, the stiffness matrix.

$$[K_f] = \begin{bmatrix} [R_w] & 0 & 0 & 0 & 0 \\ 0 & [R_w] & 0 & 0 & 0 \\ 0 & 0 & [R_w] & 0 & 0 \\ 0 & 0 & 0 & [R_w] & 0 \\ 0 & 0 & 0 & 0 & [R_w] \end{bmatrix}_{nxn} \quad \text{... (26)}$$

where,

$$[R_w]=\begin{bmatrix} K_{f1} & 0 & 0 \\ 0 & K_{f2} & 0 \\ 0 & 0 & K_{f3} \end{bmatrix}$$

In polar cylindrical coordinates:

$$K_{f1}=\int_{-1}^{+1}\int_{-1}^{+1}\int_{-1}^{+1} N_i.K_z.r\det J d\xi d\eta d\zeta$$

$$K_{f2}=\int_{-1}^{+1}\int_{-1}^{+1}\int_{-1}^{+1} N_i.K_r.r\det J d\xi r\, \eta d\zeta \qquad \ldots(27)$$

$$K_{f3}=\int_{-1}^{+1}\int_{-1}^{+1}\int_{-1}^{+1} N_i.K_y.r\det J d\xi r\, \eta d\zeta$$

The element stiffness matrix for the plate –foundation system is given as:

$$[K]= [K_P] + [K_f] \qquad \ldots (28)$$

The finite element methods in polar cylindrical coordinates are used to analyze circular plate by using 9 isoparametric plate bending elements with 8 nodes over a quarter of the plate or 9 isoparametric brick elements with twenty nodes. The mesh of the finite element is shown in figure (4).

APPLICATIONS

Two cases of thick circular plates on elastic foundations are considered in this paper. The cases are a simply supported and a fixed edge plate under uniform distributed load as shown in figure (5).

DISCUSSION

1. For the simply supported edge circular plate, figures (6) and (7) show the deflection profiles and bending moment diagram in r-direction by both the finite difference [Al-Azzawi (1995) [2]] and the present study. The results show good agreement by these two methods. The difference in central deflection is 1.53% and in central moment is 0.99 % in case of plate bending element and the difference in central deflection is 1.42 % and in central moment is 0.39 % in case of brick element. The difference in results with the exact solutions in central deflection is 0.36 % and in central moment is 0.57 % in case of brick element [15].

2. For the clamped edge plate figures (8) and (9) show the deflection profiles and the bending moment diagram in r-direction by both the finite difference [Al-Azzawi (1995) [2]] and the present study. The difference in central deflection is

1.75 % and in central moment 0.68 % in case of plate bending element and the difference in central deflection is 1.74 % and in central moment 0.57 % in case of brick element. The difference between the present study and the exact solutions in central deflection is 0.79 % and in central moment 0.35 % in case of brick element [15].

Parametric Study

To study the effects of elastic foundations and thickness on the behavior of thick circular plates, a simply supported thick plate with is studied ($K_r=K_\theta$ =20000 kN/m^3) as shown in figure (10). The loading was taken to be uniformly distributed load (q=25 kN/m^2). The effects of variation of vertical and horizontal subgrade reactions on the results of central deflections and bending moments of thick circular plates are considered. The following points are concluded from the study of the variation of vertical and horizontal subgrade reactions.

- To show the effect of variation of vertical subgrade reaction on the results, a circular plate with clamped edge and resisted by vertical subgrade reaction of various values (neglecting the effect of frictional restraints) are studied. Figures (11) and (12) show the variation of the vertical subgrade reaction on the central deflection and bending moment. From these figures the central deflection and central moment will

decrease as the vertical subgrade reaction is increased because of increasing foundation stiffness (resistance to deflection). It was found that by increasing the vertical subgrade reaction from (0.0 to 30000 kN/m^3), the central deflection is decreased by 0.20 % and the central moment is decreased by 0.25 % [1].

- To show the effect of variation of horizontal subgrade reaction, a simply supported thick plate with vertical subgrade reaction (K_z=10000 kN/m^3) and horizontal subgrade reactions of various values of (K_r and K_θ) are considered. Figures (13) and (14) show the variation of horizontal subgrade reaction (K_r and K_θ) with central deflection and central bending moment. From these figures, a reduction on central deflection and bending moment occurs as the horizontal subgrade reactions are increased. It was found that by increasing the horizontal subgrade reaction from (0.0 to 30000 kN/m^3), the central deflection is decreased by 0.34125% and the central moment by 0.43383% [1].
- To study the effect of thickness (or stiffness) of plate on the results of central deflection and central moment, a simply supported plate with various thicknesses is considered. Figures (15) and (16) show the effect of variation of thickness of the plate on central deflection and bending moment of the thick circular plate. From these figures, the central deflection

will decrease as the thickness of the plate is increased because the stiffness of plate increased. But, the central resisting moment will increase as thickness of the plate increased because of increasing stiffness. It was found that by increasing the thickness of the thick plate from (0.15 to 0.3 m), the central deflection is decreased by 96.21 % and the central resisting moment is increased by 75% [1].

CONCLUSIONS

1. The results from the finite element method are plotted with the results by finite differences. Good agreement is obtained between these methods.
2. The effect of distributed moments are small on transverse deflections of plates and on stress resultants.
3. The effect of varying the modulus of elastic foundation on the deflections and internal stress resultants of thick plates becomes slowly insignificant as the thickness increase.
4. The effect of thickness (stiffness) of plates on deflection is found to be more significant than the effect on stress resultants.

REFERENCES

1) Al-Allaf, M. H., "Three Dimensional Finite Element Analysis of Thick Plates on Elastic Foundations", M.Sc. Thesis, Faculty of Engineering, Al-Nahrain University, (2005).

2) Al-Azzawi, A. A., " Thick Circular Plates on Elastic Foundations", M.Sc. Thesis, Faculty of Engineering, Al-Nahrain University, (1995).

3) Chakravorty, A.K.and Ghosh, A.," Finite Difference Solution for Circular Plates on Elastic Foundations", International Journal for Numerical Methods in Engineering, Vol.9, pp.73-84, (1975).

4) Frederick, D., "On Some Problems in Bending of Thick Circular Plates on an Elastic Foundation", ASME (Trans.) Journal of Applied Mechanics, Vol.123, pp.195-200, (1956).

5) Hinton, E. and Owen, D.R.J, "Finite Element Programming ", Academic Press London, (1977).

6) Hinton, E. and Owen, D.R.J., "An Introduction to the Finite Element Computations" pineridge Press limited, Swansea, U.K, (1979).

7) Levinson, M., ,"An Accurate, Simple Theory of Statics and Dynamics of Elastic Plates", Mechanics Research Communications, Vol.7, pp.343-355, (1980).

8) Liu, X and, Solecki, "Green's Function for an Infinite Elastic Plate on Winkler's Foundation "ASME Journal of Engineering Mechanics, VOL.127, No.3, March, (2001).

9) Mindlin, R., "Influence of Rotary Inertia and Shear on Flexural Motions of Isotropic Elastic Plates", ASME, Journal of Applied Mechanics, VOL.18, March, pp.31-38, (1951).

10) Naghdi, P.M.and Rowely, J.C., "On the Bending of Axially Symmetric Plates on Elastic Foundations", Proc.1st Midwestern conf. on solid Mech., Univ.of Illinois, pp.119-123, (1953).

11) Perakatte, G.J. and Lehnhoff, T.F., "Flexure of Symmetrically Loaded Circular Plates Including the Effect of Transverse Shear", ASME, Journal of Applied Mechanics,Vol.101,pp.1036-1041, (1971).

12) Reissner, E., "The Effect of Transverse Shear Deformation on the Bending of Elastic Plates", ASME, Journal of Applied Mechanics, Vol.12, pp.69-77, (1945).

13) Selvadurai, A.P.S., "Elastic Analysis of Soil-foundation Interaction", Elsevier Scientific Publishing company, (1979).

14) Schmidt, R., " A Refined Nonlinear Theory of Plates with Transverse Shear Deformation", International Journal for Numerical Methods in Engineering ,Vol.1,PP.23-24, (1977).

15) Timoshenko, S.and Woinowisky-Krieger, s., "Theory of Plates and Shells", McGraw-Hill, New York, (1959).

Table (1): Shape Functions for Twenty Node Isoparametric Brick Element.

Local node number	ξ_i	η_i	ζ_i	$N_i(\xi,\eta,\zeta)$
i=1,3,5,7,13, 15,17,19	± 1	± 1	± 1	$\frac{1}{8}(1+\xi_i\zeta)(1+\eta_i\eta)(1+\zeta_i\zeta)(\xi_i\xi+\eta_i\eta+\zeta_i\zeta)$
i=2,6,14,18	0	± 1	± 1	$\frac{1}{4}(1-\xi^2)(1+\eta_i\eta)(1+\zeta_i\zeta)$
i=9,10,11,12	± 1	0	± 1	$\frac{1}{4}(1+\xi_i\xi)(1-\eta^2)(1+\zeta_i\zeta)$
i=4,8,16,20	± 1	± 1	0	$\frac{1}{4}(1+\xi_i\xi)(1+\eta_i\eta)(1-\zeta^2)$

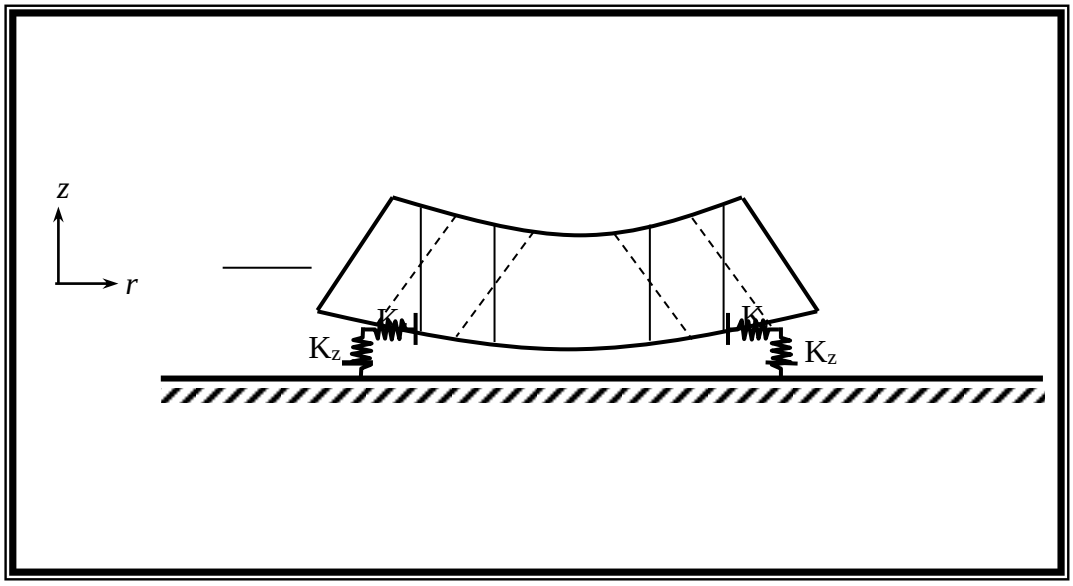

Figure (1): Winkler Compression and Friction Model.

Polynomial	Linear	Quadratic
Element	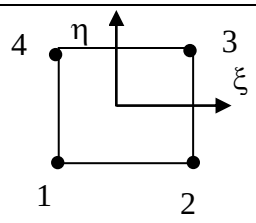	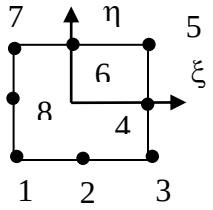

Figure (2): Types of Two-dimensional Isoparametric Elements for Thick Plates.

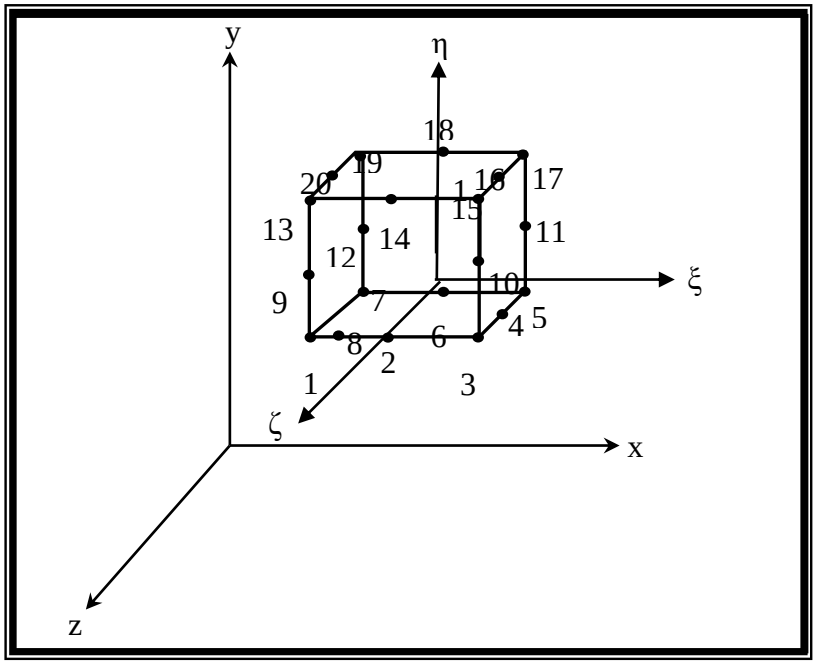

Figure (3): 20-node Isoparametric Brick Element.

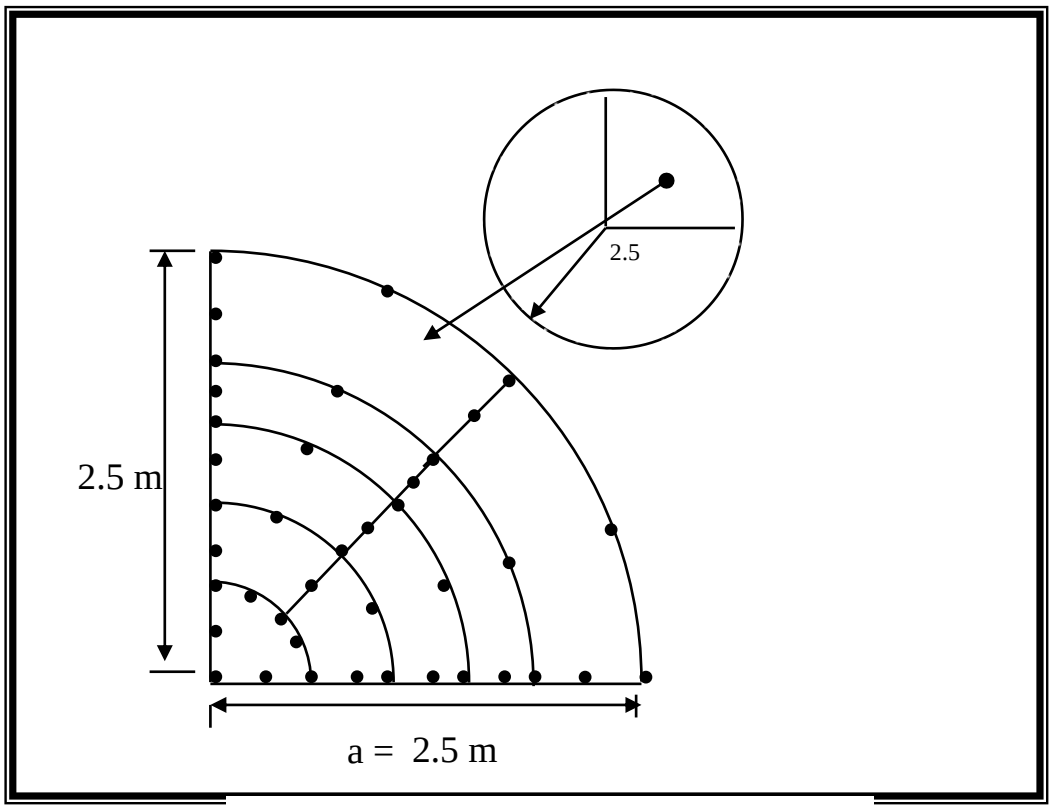

Figure (4): Finite Element Mesh.

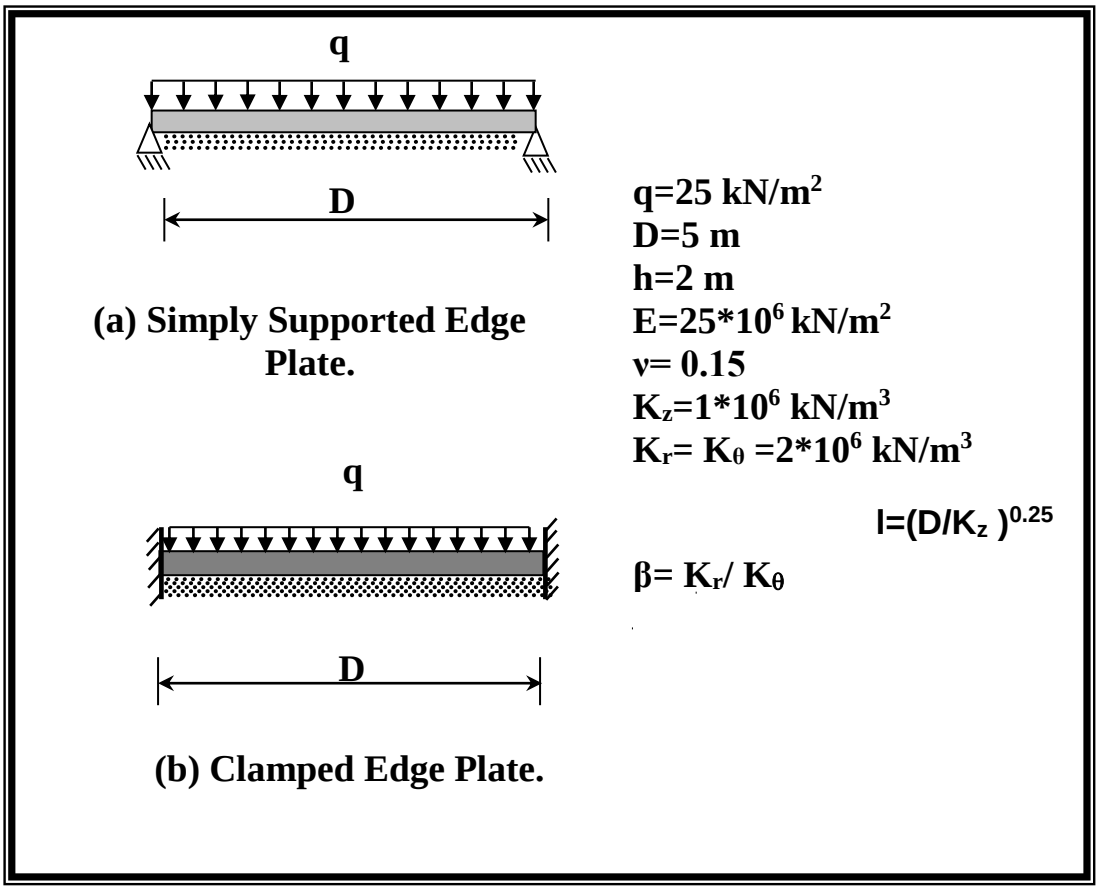

Figure (5): Circular Plate Geometry and Loading.

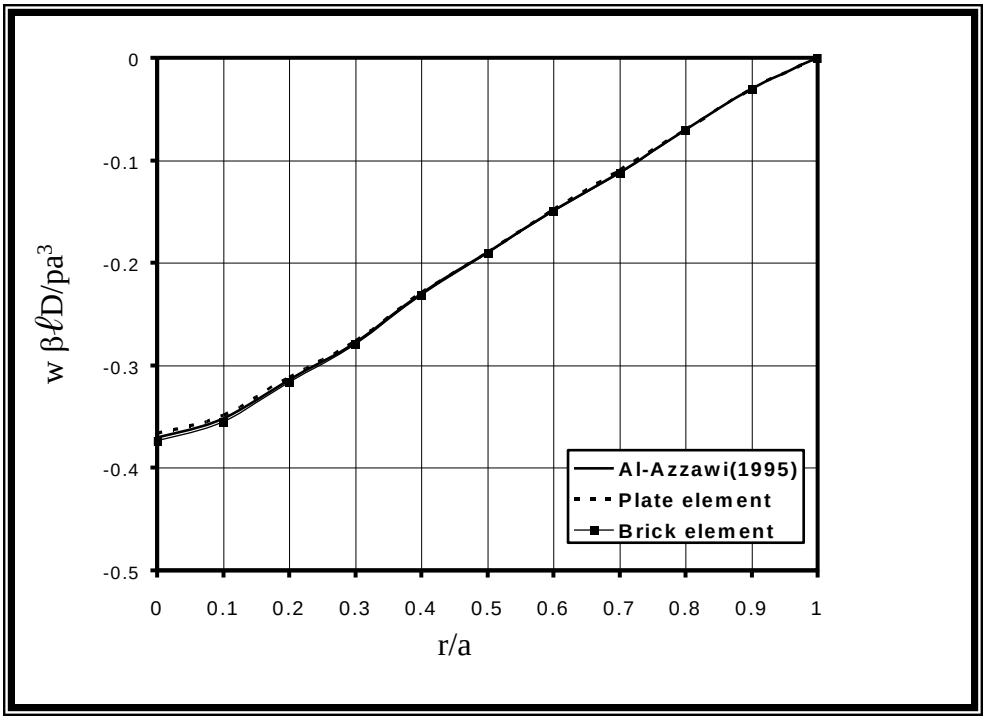

Figure (6): Deflection Profile in r- Direction for Simply Supported Thick Circular Plate.

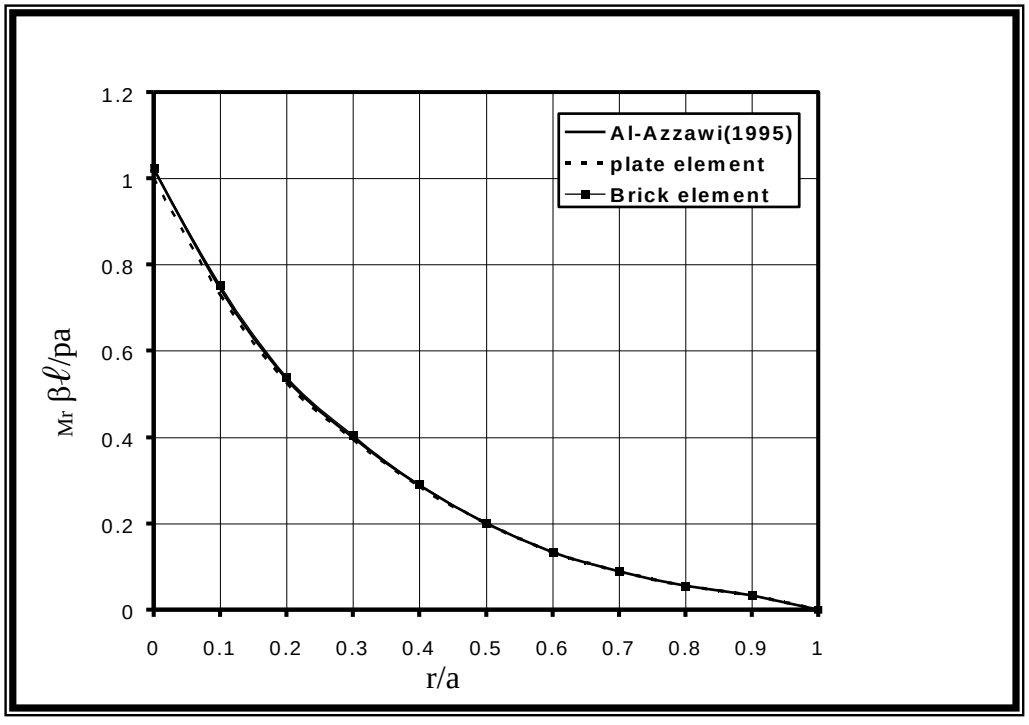

Figure (7): Bending Moment (M_r) Diagram for Thick Simply Supported Circular Plate.

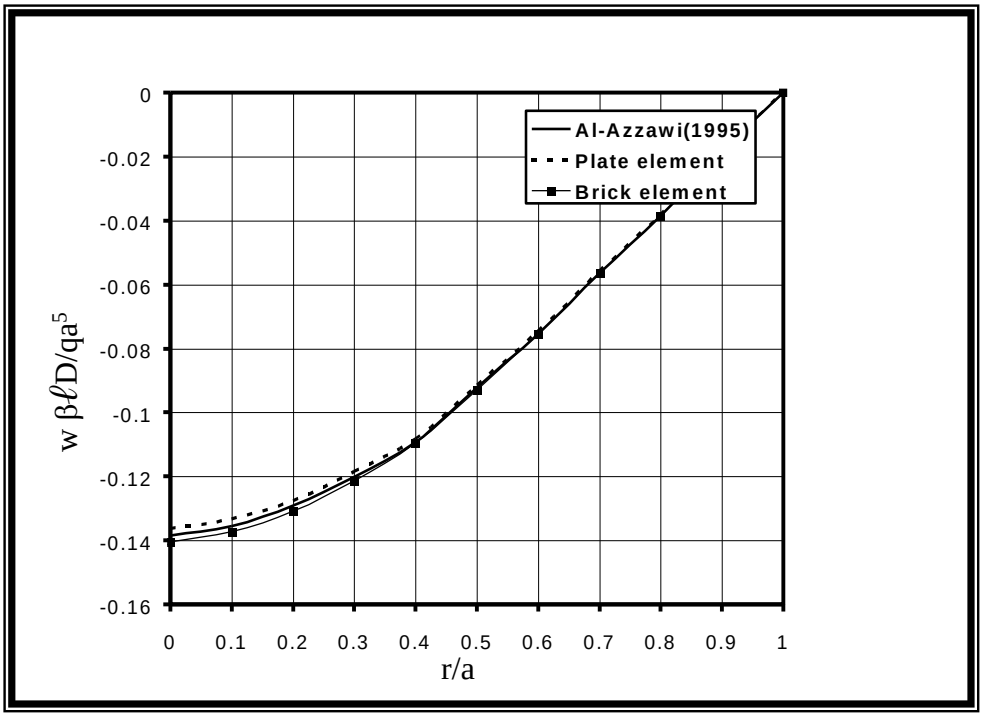

Figure (8): Deflection Profile in r- Direction for Clamped Thick Circular Plate.

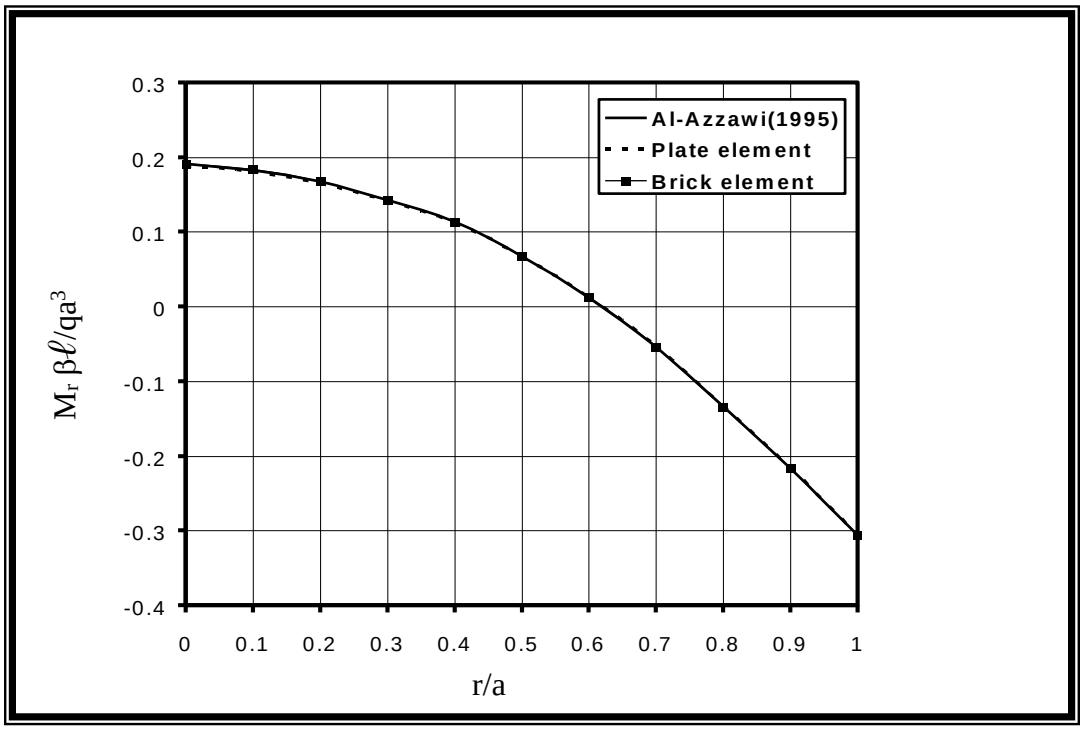

Figure (9): Bending Moment (M_r) Diagram for Clamped Thick Circular Plate.

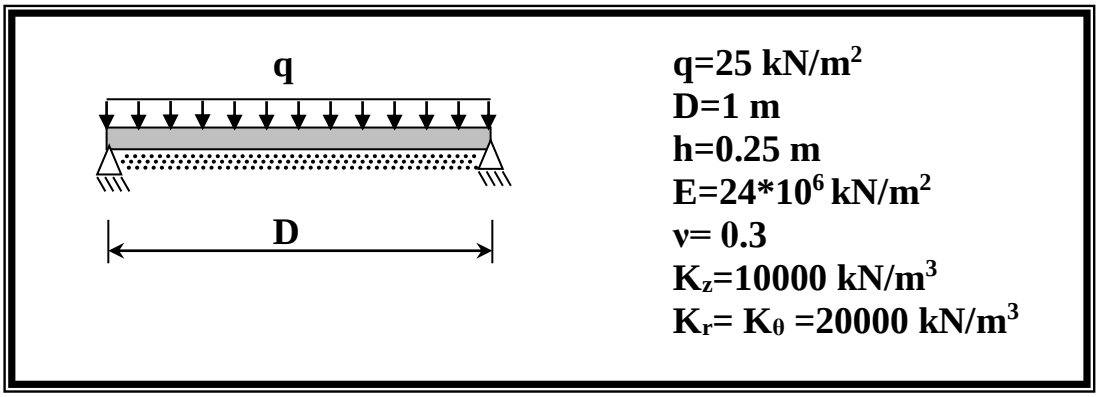

Figure (10): Circular Plate Properties and Loading.

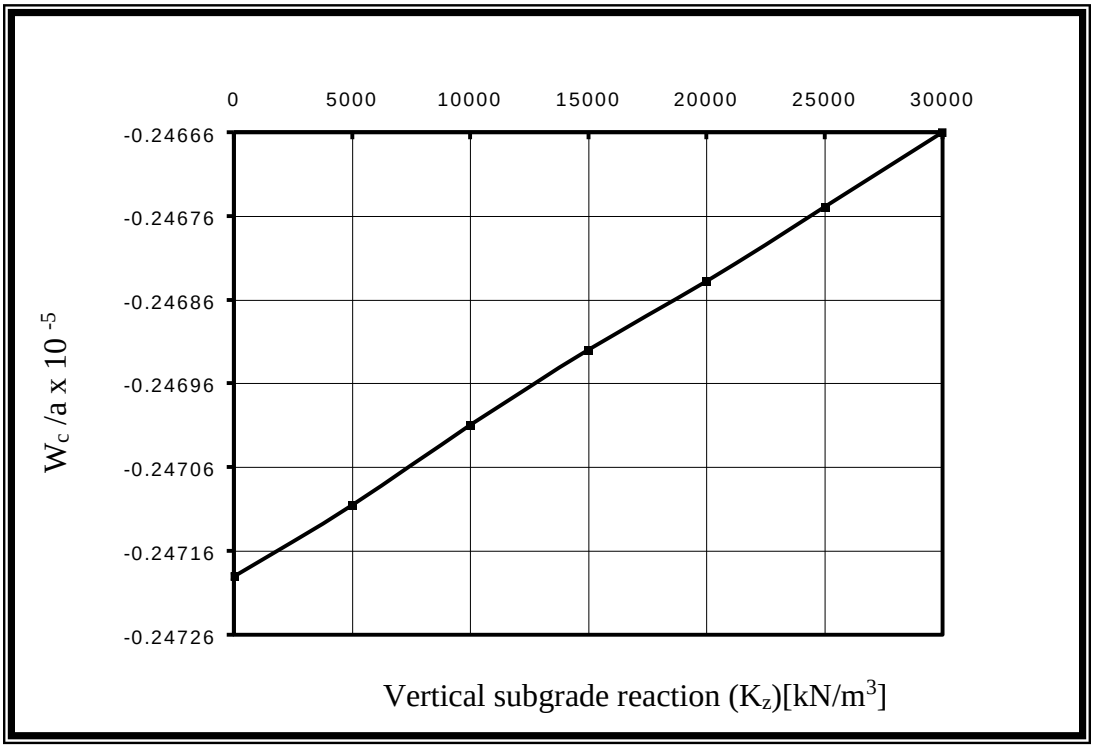

Figure (11): Effect of Vertical Subgrade Reaction on Central Deflection of Clamped Circular Plate.

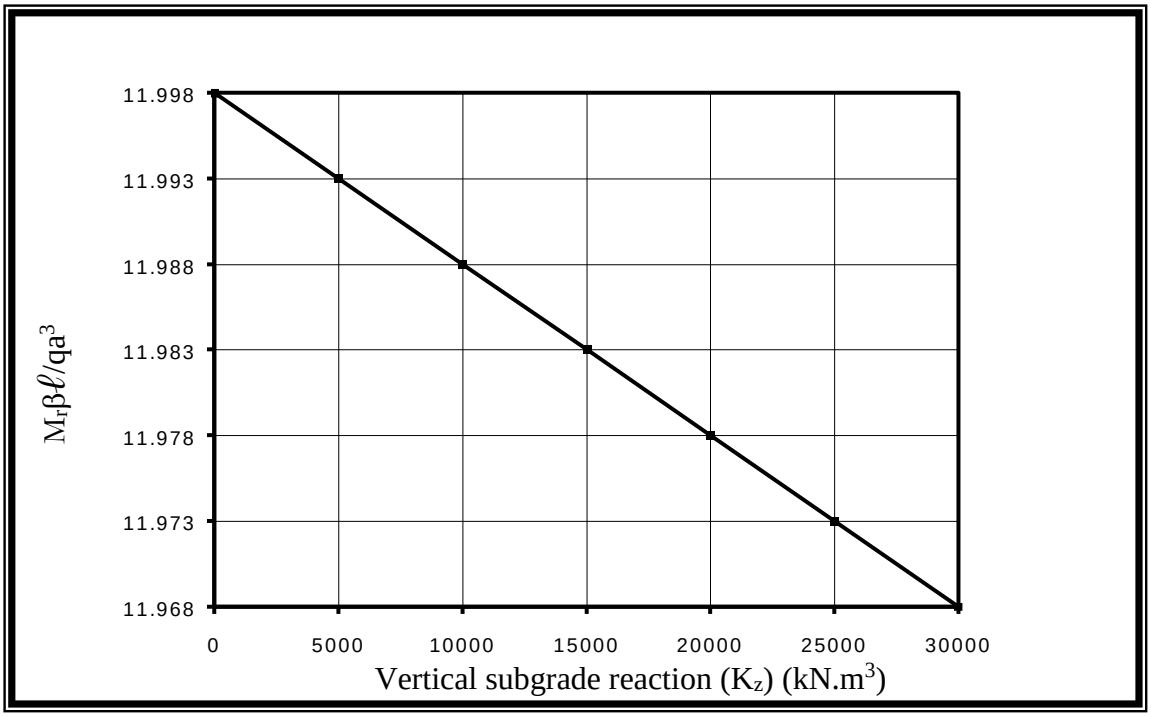

Figure (12): Effect of Vertical Subgrade Reaction on Central Moment of Clamped Circular Plate.

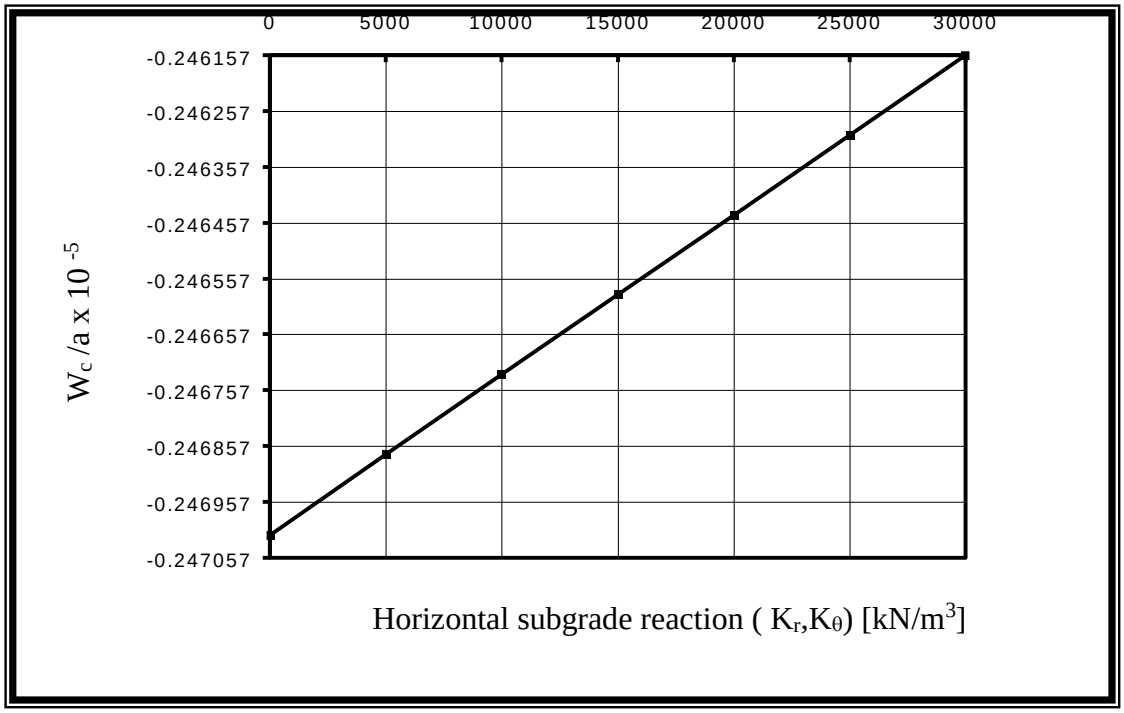

Figure (13): Effect of Horizontal Subgrade Reaction on Central Deflection of Clamped Circular Plate.

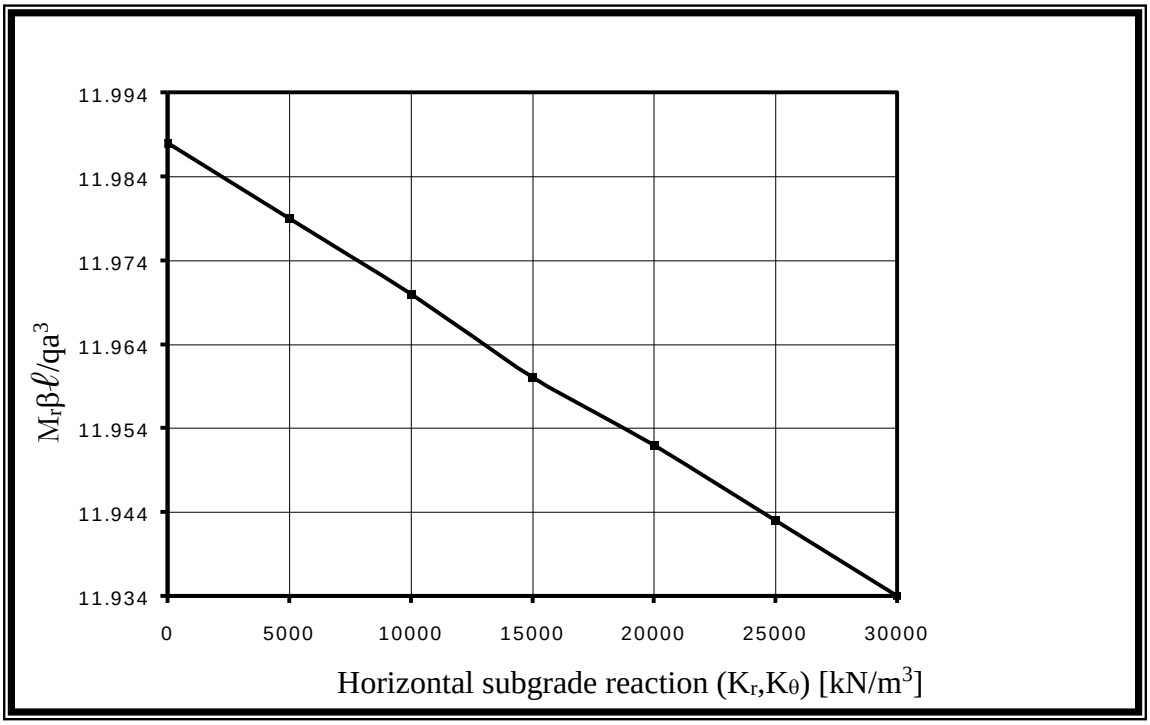

Figure(14): Effect of Horizontal Subgrade Reaction on Central Moment of Clamped Circular Plate.

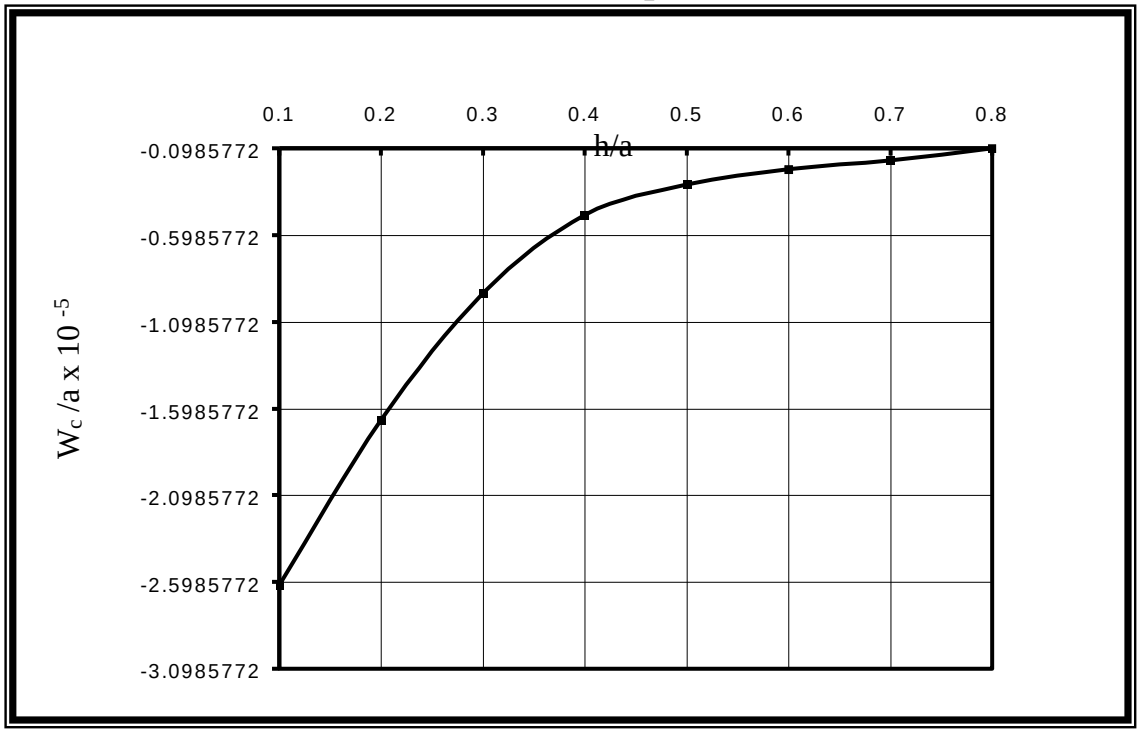

Figure (15): Effect of Thickness on Central Deflection of Clamped Thick Circular Plate.

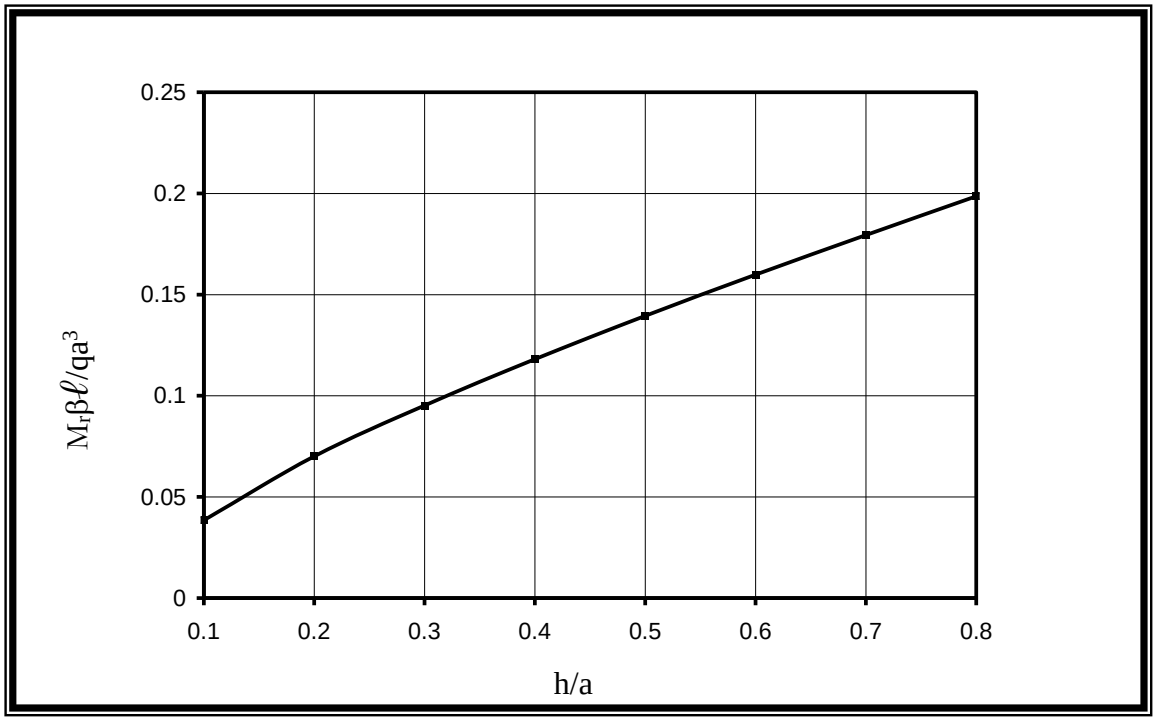

Figure (16): Effect of Thickness in Central Moment of Clamped Thick Circular Plate.

التحليل بالعناصر المحددة للالواح الدائرية السميكة والمسندة علي اسس مرنة

د. رياض جواد عزيز — **استاذ مساعد**

د. عادل عبدالامير العزاوي — **مدرس**

قسم الهندسة المدنية –جامعة النهرين

مصطفى حميد العلاف

باحث

قسم الهندسة المدنية –جامعة النهرين

الخلاصة

هذا البحث يتناول دراسة التصرف الخطي المرن للصفائح السميكه الدائريه المسنده على اسس مرنه من نوع ونكلرمع الاخذ بنظر الاعتبار مقاومات الانضغاط والاحتكاك بين التربه والصفائح . تم استخدام طريقة العناصر المحدده(عنصر الصفيحة السميكة والعنصر الطابوقي) لحل مجموعة من المسائل التي سبق وان حلت بطريقة الفروق المحددة وقد وجد ان هنالك توافق جيد مما يدل على كفاءة الطريقة المستخدمة.